**Xinsheng Gao**
e-mail: xinsheng.gao@integris-health.com

**Youdan Wang**
e-mail: kwang@houghearinstitute.com

**Kejian Chen**
e-mail: kejian.chen@integris-health.com

Hough Ear Institute,
INTEGRIS Health,
3400 Northwest 56th Street,
Oklahoma City, OK 73112

**Brian P. Grady**
School of Chemical, Biological and Materials Engineering,
University of Oklahoma,
100 East Boyd,
Norman, OK 73019
e-mail: bpgrady@ou.edu

**Kenneth J. Dormer**
Department of Physiology,
University of Oklahoma Health Sciences Center,
940 Stanton L. Young Boulevard,
Oklahoma City, OK 73104
e-mail: kenneth-dormer@ouhsc.edu

**Richard D. Kopke**[1]
Hough Ear Institute,
INTEGRIS Health,
3400 Northwest 56th Street,
Oklahoma City, OK 73112
e-mail: rkopke@houghearinstitute.com

# Magnetic Assisted Transport of PLGA Nanoparticles Through a Human Round Window Membrane Model

*The lack of an effective method for inner ear drug delivery is a clinical problem for the prevention and treatment of hearing loss. With technology advances in nanomedicine and the use of hydrogels, more drug delivery options are becoming available. This study tested the feasibility of using a tripartite layer round window membrane (RWM) model to evaluate the effectiveness of a magnetic assisted transport of poly(lactic-co-glycolic acid) (PLGA)/superparamagnetic iron oxide nanoparticles (SPIONs). A RWM model was constructed as a three-cell-layer model with epithelial cells cultured on both sides of a small intestinal submucosal (SIS) matrix with fibroblasts seeded within the matrix. PLGA encapsulated coumarin-6/SPION nanoparticles 100 nm in diameter were formulated by an oil-in-water emulsion/solvent evaporation method and pulled through the RWM model using permanent magnets with a flux density 0.410 T at the pole face. Independent variables such as external magnetic force and exposure time, composition of hyaluronic acid (HA) hydrogel suspending media, and particle characteristics including magnetic susceptibility were studied. Magnetic assisted transport of coumarin-6 labeled magnetic nanoparticles through the RWM inserts increased 2.1-fold in 1 h compared with the controls. HA hydrogel did prevent particle accumulation on the surface of RWM in a magnetic field but also impaired the mobility of these particles. Greater particle susceptibility or stronger external magnetic fields did not significantly improve the transmembrane transport. A RWM model was designed consisting of a SIS membrane and three co-cultured layers of cells, which was structurally and physically similar to the human. PLGA particles (100 nm) with encapsulated ~15 nm SPIONs were transported through this model with the assistance of an external magnet, allowing quantitative evaluation of prospective targeted drug delivery through the RWM via the assistance of a magnetic field.* [DOI: 10.1115/1.4002043]

*Keywords: SIS membrane, inner ear drug delivery, poly(lactic-co-glycolic acid), superparamagnetic nanoparticles, hyaluronic acid hydrogel*

## 1 Introduction

Treatment of auditory and vestibular dysfunction is becoming increasingly dependent on targeted inner ear drug delivery. Recent advances in molecular therapy and nanotechnology have stimulated the development of a variety of delivery methodologies involving both transtympanic and direct intracochlear infusions [1,2]. Hearing loss is a major public health problem, and its treatment with traditional therapy strategies is often unsuccessful due to limited drug access to the cochlea because of the blood-labyrinthine barrier. Drug-carrying nanoparticles may help resolve this problem because they allow for quantifiable and controlled drug release, with the potential for targeting specific cell populations, and, in some instances, can be imaged in vivo [3].

Nanoparticles (natural and synthetic) are capable of physiologically traversing the round window membrane (RWM) and cochlear membranous partitions and are likely to become useful drug delivery platforms. Tamura et al. [4] found rhodamine-encapsulated poly(lactic-co-glycolic acid) (PLGA) nanoparticles in basal and middle portions of the scalae tympani after application to the guinea pig RWM via gel foam. Nanoparticles have been demonstrated to readily cross the RWM and quickly incorporate into membranes and cells of the organ of Corti. Ge et al. [5] investigated augmentation of RWM transfer with magnetic fields using PLGA-encapsulated iron oxide nanoparticles placed on the RWM in chinchilla. Nanoparticles were subsequently identified in the scalae tympani and vestibuli, the stria vascularis, and within the organ of Corti including inner and outer hair cells and supporting cells. The mechanisms of transport have not been fully elucidated although particle size has been shown to be important in diffusion and transport across membranes in general.

The round window membranes of humans, monkeys, and rodents have comparable ultrastructures, which include three basic layers: an outer epithelium, a middle layer of connective tissue, and an inner epithelium. Interspecies variations are mainly in terms of thickness, being thinnest in rodents and thickest in humans [6]. Layers of the round window participate in absorption and secretion of substances to and from the inner ear, and the entire membrane could play a role in the drug delivery system of the ear [7,8]. Our round window membrane model is a three-layer in vitro model of the human round window membrane and contains epithelial cells cultured on both sides of a porcine small intestinal submucosal (SIS) collagen matrix (Cook Biotech) with fibroblasts (Swiss 3T3) seeded in between the epithelial layers [9].

Magnetite-PLGA superparamagnetic nanoparticles with fluorochrome coumarin-6 labeling were evaluated for transmembrane transport using the RWM model. PLGA nanoparticles with encapsulated ~15 nm superparamagnetic iron oxide nanoparticles

[1]Corresponding author.

Manuscript received May 14, 2010; final manuscript received June 10, 2010; published online August 23, 2010. Editor: Vijay K. Varadan.

(SPIONs) were pulled through the RWM model using permanent rare earth (NdFeB) magnets with field strength of 0.410 T at the pole face. Our model is being used to quantitatively evaluate parameters that might affect the targeted delivery of therapeutics across the human RWM.

## 2 Materials and Methods

Culture media were purchased from Gibco-Invitrogen (Carlsbad, CA), including Dulbecco's modified eagle medium (DMEM) and fetal bovine serum (FBS). Poly(D,L-lactide-co-glycolide) (50:50: lactide/glycolide, iv ~0.67 dl/g) was purchased from Absorbable Polymers International (Pelham, AL); coumarin-6 and polyvinyl alcohol (PVA) (molecular weight (MW) 30–70 kDa) were purchased from Sigma Chemical Co (St. Louis, MO). Oleic acid-coated superparamagnetic iron oxide nanoparticles were purchased from Liquid Research Ltd. (Bangor, Gwenedd, LL527 2UP, UK). Dichloromethane was purchased from VWR (Aurora, CO). Porcine SIS membranes were gifts from Cook Biotech Inc. (Lafayette, IN). Hyaluronic acid (HA) hydrogel with MW 0.75, 0.96, and 1.46 MDa were purchased from Genzyme (Cambridge, MA).

**2.1 Formulation of Magnetic Nanoparticles Containing Coumarin-6.** An oil-in-water emulsion/solvent evaporation method was used to produce coumarin-6 labeled magnetic nanoparticles. Briefly, 200 mg of PLGA with superparamagnetic iron oxide nanoparticles, at concentrations of 5 mg/ml, 10 mg/ml, 20 mg/ml, and 30 mg/ml, was dissolved in 9 ml dichloromethane. 1 ml of coumarin-6 in acetone (50 mg/ml) was mixed with the dissolved polymer solution. The mixture was added to 40 ml of aqueous solution containing 2.5% polyvinyl alcohol. The system was sonicated on ice using a probe sonicator (Ultrasonic Processor VCX-130, Sonics, CT) for 10 min at 40 W and stirred for 4–24 h to allow the organic solvents to evaporate. After synthesis, particles were isolated by centrifugation at 15,000 rpm (Beckman Optima LE-90K, Beckman Instruments Inc., Palo Alto, CA) and washed three times with nanopure water to remove any excessive coumarin, PVA, and SPIONs. Lastly, the particles were suspended in nanopure water, frozen, and lyophilized for 2 days and stored at −80°C until use. The particles consisting of PLGA polymer, encapsulated SPIONs, and a payload (coumarin-6) will be referred to as coumarin labeled magnetic multifunctional nanoparticles (CMNPs) in this paper [10].

### 2.2 Particle Characterization

*2.2.1 TEM.* Particle size, aggregation state, and the distribution of SPIONs inside PLGA nanoparticles were characterized by transmission electron microscopy (TEM) (H7600 electron microscope, Hitachi, Pleasanton, CA). A drop of particle suspension was placed on a formvar-coated copper grid for 30 s. Then, the liquid sample was wicked off and rinsed three times with one drop of deionized water. The sample was then stained with a drop of uranyl acetate for 10 s.

*2.2.2 Particle Sizing and Zeta Potential.* The hydrodynamic particle size in water was determined by dynamic light scattering (DLS) (Brookhaven 90Plus, Holtsville, NY). The surface charge of particles was evaluated using ZetaPlus (Brookhaven Zeta PALS, Long Island, NY). All samples were suspended in nanopure water, and ten measurements were taken for each sample.

**2.3 Cell Culture.** Madin–Darby canine kidney (MDCK) epithelial cells and Swiss 3T3 fibroblast cells were purchased from American Type Culture Collection (ATCC). MDCK cells were used between passages 16 and 40, and 3T3 cells were between passages 7 and 35. Cells were cultured in 100 mm culture dishes in DMEM supplemented with 10% FBS for MDCK and 3T3 cells. Cells were maintained at 37°C under 5% $CO_2$. The medium was changed every other day until the cells reached confluence. Cells were then washed with phosphate buffered saline (pH7.4) (PBS) and detached using trypsin-(2,2′,2″,2‴-(ethane-1,2-diyldinitrilo) tetraacetic acid (EDTA) and then cultured on the SIS membrane in plastic inserts that fit into 24-well culture plates. Media were changed on the inserts every 2 days. Cells that were not used for experimentation were cultured in 100 mm culture dishes and re-incubated at 37°C under 5% $CO_2$. The seeding density was $4.75\times10^5$ cells/cm$^2$ [9].

**2.4 Transepithelial Electrical Resistance.** Transepithelial electrical resistance (TEER) was measured to confirm the confluence of these polarized epithelial cells [11]. The resistance of the cultured SIS membrane was measured using an epithelial volt-ohmmeter (EVOM, World Precision Instruments, New Haven, CT). TEER was determined by applying a square wave alternating current of ±20 $\mu$A at 12.5 Hz with a silver electrode and measuring the potential difference with a silver/silver chloride electrode using the EVOM at 37°C in tissue culture media (DMEM with 10% FBS and 1% PS).

**2.5 Magnetic Assisted Transport Across the RWM Model.** Magnetic assisted transport (MAT) was quantified by measuring the coumarin fluorescence intensity of CMNPs collected on the underside of the RWM inserts. The amount of particles pulled through the RWM was compared with and without the use of underlying magnets. To grow the model, MDCK cells were first seeded on the serosal side of the SIS membrane at a seeding density of $4.4\times10^5$ cells/cm$^2$. Swiss 3T3 fibroblasts were seeded on the mucosal side of the SIS membrane at a seeding density of $1.8\times10^3$ cells/cm$^2$. The fibroblasts were allowed 2 days to penetrate into the SIS membrane. Then, MDCK cells were cultured on the mucosal side of the SIS membrane at a seeding density of $4.4\times10^5$ cells/cm$^2$. Magnetic PLGA nanoparticles labeled with coumarin-6 were used in the experiments. Typically, these particles were suspended in PBS (pH 7.4) at 0.5 mg/ml. For particles embedded in different HA hydrogels, HA hydrogels were evenly spread on the wall of 15 ml sterile tubes and mixed with the homogeneous particle solution in PBS. The mixture was shaken for 4 h before applying onto the RWM inserts. All experiments were done at day 5 of cell culture of the last layer of cells cultured on the RWM model. The magnetic cylinders (MagStar Technologies, Hopkins, MN) were $6.35\times6.35$ mm$^2$, and the centers of adjacent magnets were 2 cm apart. A plastic molding ($12.8\times8.6\times3.1$ cm$^3$) held the magnets directly under a 24-well culture plate. Magnetic flux density was measured using a Gauss meter model 5080 (SYPRIS, Orlando, FL).

The suspensions of transported particles were collected and freeze-dried, and finally, coumarin-6 was extracted with 1 ml chloroform. The fluorescence intensity of transported coumarin-6 was measured by an SLM 8100 photon-counting spectrofluorometer (ISS Inc., Champaign, IL) at a wavelength of 500 nm under an excitation wavelength of 430 nm [12]. SIGMAPLOT was used to generate the figures, and all comparisons were performed using paired, two-tailed Student's $t$-tests. Results are expressed as means ± SEM (standard error of the means).

## 3 Results

**3.1 Characterization of the Particles.** The CMNPs were formulated by the single emulsion/solvent evaporation method and were analyzed. They were 100 ± 36 nm in diameter, and SPIONs were evenly distributed inside the PLGA particles, as qualitatively assessed by TEM (Fig. 1). Their hydrodynamic size was 250 ± 52 nm measured by DLS. The zeta potential of these particles was −27 ± 3 mV evaluated by ZETAPLUS.

**3.2 Transport Time.** To determine the best time point for the maximum transmembrane transport of CMNPs, we carried out the magnetic assisted transport on RWM inserts for different time points, 30 min, 1 h, and 2 h. The amounts of coumarin inside the transported CMNPs were analyzed by an ISS photon-counting

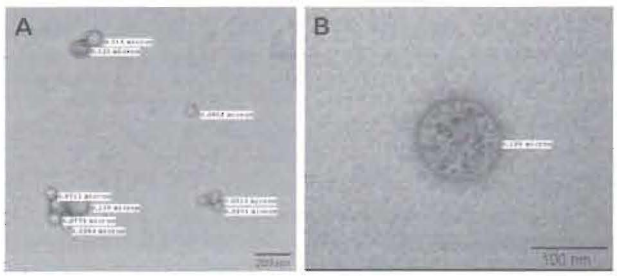


**Fig. 1 TEM images of coumarin labeled magnetic PLGA nanoparticles. Magnifications in A and B were 20,000× and 100,000×, respectively. The dark spots in B were SPIONs evenly spread inside the PLGA particles.**

spectrofluorometer (Fig. 2). It was found that the time point to generate the largest difference between MAT and control samples was 1 h. The ratios of magnet transport samples to nonmagnet controls were 2.1 for 1 h, 1.71 for 30 min, and 1.56 for 2 h. The fraction of particles crossing the membrane in 1 h was approximately 0.1%, as discussed in more detail below.

**3.3 Hydrogel Composition.** We noticed that the paramagnetic nanoparticles would form clusters at the surface of the RWM inserts in as short as 10 min, and this agglomeration may decrease the ability of the particles to enter and cross the membrane. Our hypothesis was that particles are transported much faster through the low viscosity water and collect at the interface between the water and the high viscosity RWM insert. Hence, the nanoparticles were suspended in HA hydrogel matrices, which might prevent the accumulation of nanoparticle clusters at the interface because the viscosities are better matched, and improve the transmembrane permeability. CMNPs (0.5 mg/ml) were dispersed in the same concentration (9 mg/ml) of different cross-linked hydrogels (0.75 MDa, 0.96 MDa, and 1.47 MDa) and were evaluated with the RWM MAT analysis. The transport of CMNPs was decreased with increasing molecular weight of the hydrogels; the ratios of magnet assisted transport samples to nonmagnet controls were between 1.37 and 1.41 (Fig. 3). The amount of CMNPs that were transported across the membrane was 0.095 $\mu$g (out of 100 $\mu$g added to the retentate side of the RWM model) if CMNPs were embedded in the HA hydrogels, while the amount was 0.15 $\mu$g (e.g., 0.15%) if CMNPs were suspended in PBS only. Visible particle agglomeration on the surface of the RWM was not

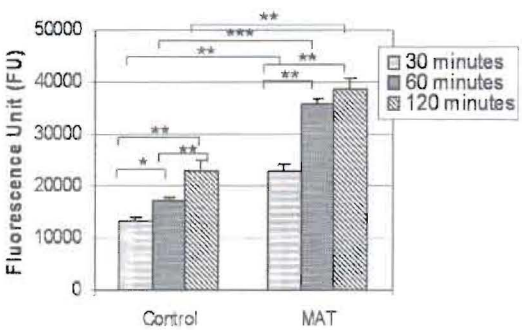


**Fig. 2 The time course of the RWM MAT of CMNPs. The fluorescence intensity of coumarin-6 extracted from the magnet assisted transports and controls without magnetic flux was measured at 500 nm using an excitation wavelength of 430 nm. The significance of differences was compared within all control and MAT samples and also between control and MAT samples. The results were analyzed using Student's paired two-tailed *t*-tests. Results are expressed as means±SEM. Asterisks *, **, and *** represent p<0.05, p<0.01, and p<0.001, respectively.**

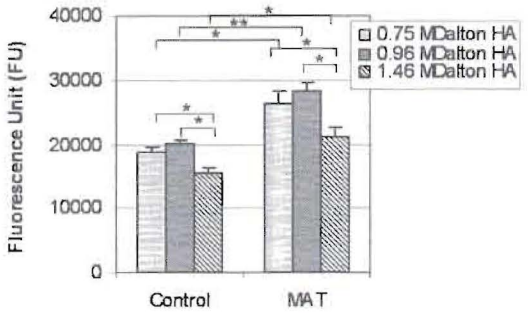


**Fig. 3 Bar graphs of the RWM MAT of CMNPs suspended in hydrogel of different molecular weight. The transmembrane permeability data were shown for CMNPs suspended in 9 mg/ml hydrogels with MW 0.75 MDa, 0.96 MDa, and 1.47 MDa. The significance of differences between control and MAT samples was obtained by Student's paired two-tailed *t*-tests. Results are expressed as means±SEM. Asterisks * and ** represent p<0.05 and p<0.01, respectively.**

detected, but the high viscosity matrices also impaired the transmembrane permeability of CMNPs in the time window (1 h) we tested.

**3.4 Hydrogel Concentration.** To avoid the negative effect of HA hydrogel on MAT of CMNPs, transmembrane permeability of CMNPs suspended in lower concentrations of HA hydrogel was tested. CMNPs (0.5 mg/ml) were suspended in a series of concentrations of hydrogel (MW 0.75 MDa) solutions (0.67 mg/ml, 2 mg/ml, and 6 mg/ml). MAT on RWM inserts was carried out with or without the permanent magnet array with a flux density of 0.410 T. The results indicated that the 0.67 mg/ml HA embedded CMNPs gave the best transmembrane permeability. The ratio of magnet assisted transport samples to nonmagnet controls was about 2.1 (Fig. 4); i.e., approximately 0.15% of the total that was added crossed the membrane in the former case. The transport of CMNPs was decreased with increasing hydrogel concentrations; the ratios were 1.63 and 1.54, respectively (Fig. 4).

**3.5 Nanoparticle Magnetic Susceptibility.** In order to increase the transmembrane transport of the paramagnetic nanoparticles, we assumed that improving the susceptibility of particles to external magnetic fields by loading more magnetite into the polymeric nanoparticles might result in better MAT of coumarin-6 nanoparticles. We synthesized PLGA nanoparticles with concentrations of magnetite 5 mg/ml, 10 mg/ml, 20 mg/ml, and 30 mg/ml under the same sonication conditions and obtained the CMNPs

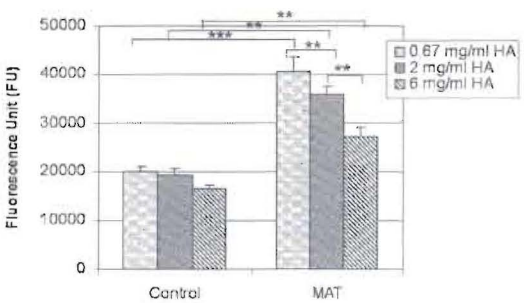


**Fig. 4 Bar graphs of the RWM MAT of CMNPs suspended in serial dilutions of hydrogel. The results indicated the transmembrane permeability data for CMNPs suspended in 0.67 mg/ml, 2 mg/ml, and 6 mg/ml hydrogel (MW 0.75 MDa). The significance of differences between control and MAT samples was obtained by Student's paired two-tailed *t*-tests. Results are expressed as means±SEM. Asterisks ** and *** represent p<0.01 and p<0.001, respectively.**

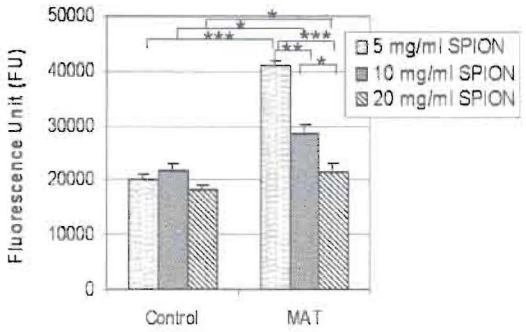


**Fig. 5 RWM MAT of CMNPs with different magnetic susceptibilities. The bar graphs show the fluorescence intensity of coumarin-6 extracted from CMNPs synthesized with 5 mg/ml, 10 mg/ml, and 20 mg/ml magnetites, respectively. The significance of differences between control and MAT samples was obtained by Student's paired two-tailed *t*-tests. Results are expressed as means±SEM. Asterisks *, **, and *** represent p <0.05, p<0.01, and p<0.001, respectively.**

with similar sizes [10,13]. The relationship between magnetite concentration in the synthesis procedure and saturation magnetization has been presented elsewhere; essentially, the saturation magnetization (emu/g) scales with magnetite concentration in solution on a line with a slope of ~0.9 [14]. Using the same data, the same linear relationship exists for magnetic susceptibility (emu/(g Oe)), with a scaling constant of about 0.015. CMNPs synthesized with 30 mg/ml magnetite could not be homogeneously dispersed and were omitted from the MAT experiment. The CMNPs synthesized with 5 mg/ml magnetite content had the best transmembrane transport; the mag/nonmag ratio was 2.06. The transmembrane transport of CMNPs with 10 mg/ml and 20 mg/ml magnetite was much lower; the mag/nonmag transport ratios were 1.32 and 1.2, respectively (Fig. 5).

**3.6 External Magnetic Field.** To identify the optimal magnetic environment for the RWM drug delivery, we investigated magnetic assisted transport of CMNPs with magnet arrays of different field strengths (0.25 T, 0.41 T, and 1.0 T). The transport ratios of CMNPs through RWM inserts under magnetic fields of 0.25 T and 0.41 T to nonmagnet controls were 2.0 and 2.2, respectively. But the stronger magnetic force of 1.0 T resulted in a lower transmembrane transport ratio for CMNPs; i.e., the ratio of magnet transport samples to nonmagnet controls was 1.44 (Fig. 6). We

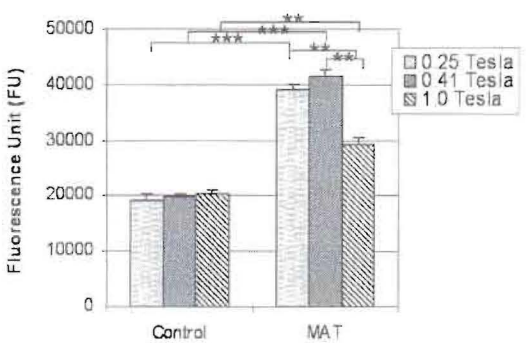


**Fig. 6 RWM magnet assisted transport of CMNPs under different magnetic fluxes. The bar graphs show the fluorescence intensity of coumarin-6 extracted from the MAT samples and control samples without magnetic flux. The results were obtained under magnetic fluxes of 0.25 T, 0.41 T, and 1.0 T. The significance of differences between control and MAT samples was obtained by Student's paired two-tailed *t*-tests. Results are expressed as means±SEM. Asterisks ** and *** represent p <0.01 and p<0.001, respectively.**

noticed that the agglomeration of CMNPs on the surfaces of RWMs occurred much more rapidly (in about 3 min) under a stronger magnetic flux intensity than under the weaker magnetic fields.

## 4 Discussion

Inner ear drug delivery methods, including single transtympanic injections, continuous infusions, and periodic infusions, have been studied extensively. Local administration of otoprotectives on the RWM represents a promising and effective alternative for drug delivery. The RWM is located in the medial wall of the inner ear, separating the middle ear from the scala tympani. The RWM behaves like a biological semipermeable membrane and has selectivity for permeability of substances. Factors such as particle size, configuration, concentration, liposolubility, electrical charge, and thickness of the membrane influence membrane permeability [15].

Animal studies have been used to explore details of drug distribution and cellular impact with acute and sustained infusions to the RWM. Coleman et al. [16] evaluated the application of a cell-permeable inhibitor of c-Jun N-terminal kinase (JNK)-mediated apoptosis, AM-111, to the RWM of noise exposed chinchilla and found that this method provided superior protection over intraperitoneal injection and continuous perfusion. Plontke et al. [17] detected a strong basal-apical concentration gradient of dexamethasone in guinea pig perilymph following administration directly onto the RWM. Kopke et al. [8] reported on the results of continuous infusion of corticosteroid via a catheter placed in the round window niche as a treatment for sudden sensorineural hearing loss.

Animal models provide essential insights to quantitatively analyze the drug distribution inside the labyrinth. But the large difference in thickness between the animal and human RWM raises more questions on the pharmacokinetics of inner ear drug delivery. The thickness of human RWM is more than 100 $\mu$m, much thicker than the RWM in rodents (chinchilla and guinea pigs' RWM are only 25–30 $\mu$m in thickness). We established the RWM model based on SIS membrane with a collagen layer of about 100 $\mu$m with epithelial cells seeded on both sides. The in vitro RWM is very cost effective and physically and structurally resembles the human RWM. We characterized the transmembrane permeability of CMNPs through the RWM inserts and found that MAT could improve the transport of nanoparticles twofold compared with control inserts.

Stabilizing matrices placed on the round window membrane for sustained passive delivery of compounds offer controlled dosing profiles. Techniques stabilizing gel matrices for passive sustained release facilitate close contact between the matrix and the RWM. This material has been used successfully in mouse studies to deliver dexamethasone to the inner ear through the RWM and has tunable delivery properties [18]. Attenuation of noise-induced hearing loss by application of recombinant human insulinlike growth factor 1 (rhIGF-1) to the RWM via hydrogel has been examined in guinea pigs and rats [19].

The observation that the application of a magnetic field only increased the transport of particles through the membrane by a factor of 2 and that the amount passing through is only roughly 0.15% of the total is surprising. This observation requires further analysis in an attempt to understand the origin of such a small transport increase with the application of a magnetic field. The velocity of a particle will be determined by when the viscous drag force is equal to the magnetic force, assuming that continuum mechanics applies. The force for the former is governed by the Stokes equation given by

$$F_d = 6\pi R_{np}\eta v \tag{1}$$

where $F$ is the viscous drag force the particle feels, $R_{np}$ is the radius of the nanoparticle, $\eta$ is the viscosity of the fluid, and $v$ is the velocity of the particle. In our situation, the magnetic force is

below that required for magnetic saturation, and hence the force is given by [14]

$$F_m = \frac{2\pi R_{np}^3 \mu_0}{3} \frac{\chi}{1+\chi/3} \nabla H^2 \quad (2)$$

where $\chi$ is the volume susceptibility of the nanoparticle and $H$ is the magnetic field strength (in SI units A/m) and $\mu_0$ is the permeability in free space ($4\pi \times 10^{-7}$ (V s)/(A m)). The measured volume susceptibility of the particles synthesized with 10 mg/ml magnetite concentration can be determined from Fig. 2 of Ref. [14] (after converting from mass to volume susceptibility, which involves multiplying by $4\pi^*$ particle density) and is equal to a value of ~0.2. With a 0.5 T magnet, a linear field decay length of 1 cm, a particle with 300 nm diameter and the viscosity of water gives a velocity of about ~0.3 mm/min. This value is approximately 0.5–1 orders of magnitude less than that observed experimentally in water; errors in the decay length and the nature of that decay could be well responsible for the error. Still, however, the formula does seem to give a reasonable representation of the velocity in water. So, why is the velocity through the model RWM so slow?

One possibility is the effective viscosity of the RWM model: The lack of transport could be due to a higher viscosity in the RWM model if the viscosity is of order 1000 times that of water or higher. However, the explanation of a higher viscosity causing reduced transport is unlikely because to view the RWM insert as a continuum is likely flawed. With a continuum viscosity of 1000 times that of water, no measurable transport of the nanoparticles across the membrane would be expected in the absence of a magnetic field if transport is via Fickian-type diffusion. Further, the fact that increasing the effective magnetic force, either by increasing magnetite concentration or by increasing the magnetic strength, did not increase the relative amount of CMNPs passing through the insert suggests a noncontinuum medium. Active modes of transport, which are well known in biological systems, could be the governing transport of the nanoparticles across the membrane. Further, given the morphology of the membrane, one would expect that a tortuous pathway would be a better description of transport through the insert.

The observation that there is a visible increased concentration of CMNPs at the RWM-hydrogel interface becomes more important if the RWM insert is not a continuum in terms of transport. Particle agglomeration almost certainly occurs at this interface. Agglomerated particles would be expected to have much more difficulty passing through a noncontinuum. If an individual particle is slowed or stopped by a barrier, then another particle approaching the barrier would lead to agglomeration, similar to a filtration process. Even in the absence of a barrier, it is possible for the application of a magnetic field to induce particle agglomeration through two mechanisms. The first is the fact that a faster moving particle (faster either because of size or because of more magnetite) could "overtake" a slower moving particle in the direction of the magnetic field gradient. Second, there is a particle-particle attractive force due to the fact that the particles are magnetic with an applied magnetic field.

To determine the nature and characteristics of agglomeration no matter what the cause, it is appropriate to consider the forces involved. The electrostatic force, which is a result of the zeta potential, is repulsive and given by

$$F_e = \frac{2\pi\varepsilon_r\varepsilon_o R_{np}\zeta^2\kappa e^{-\kappa s}}{(1+e^{-\kappa s})} \quad (3)$$

where $\zeta$ is the zeta potential, $\kappa$ is the reciprocal double layer thickness, $s$ is the particle-particle separation distance (e.g., center to center distance—diameter), and $\varepsilon_r\varepsilon_o$ is the static permittivity of water. Reasonable values for these parameters in water without electrolyte yield a force on the order of $10^{-10}$ N per particle at a separation distance on the order of $10^2$ nm. The force according to Eq. (2) gives a value of approximately $10^{-13}$ N per particle, indicating that "agglomerates" at a wall would consist of particles that are separated by hundreds of nanometers. From the viewpoint of a larger particle passing through a tortuous pathway, the fact that the particles are separated versus being close together is likely irrelevant with regard to transport since in either case the agglomerated particles are expected to be much slower than isolated particles in passing through the insert.

There is a particle-particle magnetic force that must be considered. The magnetic attractive force between particles depends on the geometry of the particles relative to the magnetic field and will be a maximum when the line that connects the center of the particles is on the same line as the magnetic field gradient and zero when the two are at right angles to one another. An upper limit on this force can be calculated by assuming saturation magnetization ($M_s$) as well as alignment of all dipole spins in each individual magnetite particle [20]:

$$F_{d-d} = \frac{24\pi\mu_0 R_{np}^6 M_s^2}{9(s+2R_{np})^4} \quad (4)$$

This force is of order of magnitude $10^{-13}$ at a distance $s$ of $10^2$ nm. Hence, this force does not alter the overall picture of agglomerates at walls consisting of particles separated by hundreds of nanometers; however, this attraction provides a reason for chainlike agglomerates due to the directional dependence of this force.

In this study, the HA hydrogel embedded CMNPs demonstrated impaired passive diffusion through the thick human RWM model at the 1 h time point. CMNPs suspended in the low concentration of HA hydrogel (0.67 mg/ml) showed the similar transport efficiency as CMNPs suspended in PBS buffer. Similarly, neither stronger magnetic flux nor higher magnetite susceptibility of nanoparticles could significantly improve the magnetic assisted crossover of PLGA magnetic nanoparticles through the RWM model. In our experience, the greatest barrier to the transmembrane permeability of magnetic nanoparticles is agglomeration that is noticeable at the RWM interface. Further studies will focus on changing the surface chemistry of the particles to perhaps take advantage of active transport mechanisms, as well as on the use of oscillating magnetic fields to hopefully improve transport.

## 5 Conclusion

Magnetite ($Fe_3O_4$), combined with the FDA approved biopolymer, PLGA, produces a versatile drug delivery platform that may be capable of directing therapeutics to a specific organ or tissue by applying a magnetic field. A major advantage of magnetic targeting of the cochlea by way of the round window membrane is that the bloodstream and removal of particles by mononuclear phagocyte cells (MPCs) do not impair the delivery, and the blood-labyrinthine barrier is bypassed. This study showed that magnetic assisted transport of CMNPs through the RWM inserts increased twofold in 1 h compared with the controls. HA hydrogel (9 mg/ml) could prevent visible particle accumulation on the surface of RWM inserts in a magnetic field, though it also impaired the permeability of these particles through the membrane, presumably because transport through the hydrogel occurs at a much slower velocity than transport through water. Greater particle susceptibility or stronger external magnetic fields cannot improve the transmembrane transport; on the contrary, they had the opposite effects on the magnetic assisted transport of CMNPs. Our investigation may be the first systematic study of transport of magnetic PLGA nanoparticles through a humanlike RWM and may shed light on improving magnetic nanoparticles for inner ear drug delivery. Factors such as delivery payload, zeta potential, size of particles, magnetic susceptibility, and other parameters should be considered when using an external magnetic vector to enhance particle delivery across a biologic membrane.

## Acknowledgment

The present work was supported by the NIH Grant No. R21-00357540, OCAST Grant No. AR082-009, and INTEGRIS Health, Oklahoma City, OK. We are grateful to Dr. Chul-Hee Choi for his help with the statistical analysis of the data and to Dr. Jianzhong Lu for his review of the manuscript. We are grateful for discussions with Dr. Isaac Rutel regarding the induced particle-particle magnetic forces. We would like to thank Cook Biotech Inc. for their generous gift of the SIS membranes. We are also indebted to Dr. J. W. Harrell (Department of Physics, University of Alabama) for his help with the measurement of the magnetic susceptibility of our CMNPs.

## References

[1] Swan, E. E., Mescher, M. J., Sewell, W. F., Tao, S. L., and Borenstein, J. T., 2008, "Inner Ear Drug Delivery for Auditory Applications," Adv. Drug Delivery Rev., **60**, pp. 1583–1599.

[2] Richardson, R. T., Wise, A. K., Andrew, J. K., and O'Leary, S. J., 2008, "Novel Drug Delivery Systems for Inner Ear Protection and Regeneration After Hearing Loss," Expert Opin. Drug Deliv., **5**, pp. 1059–1076.

[3] Wang, Z., Chui, W. K., and Ho, P. C., 2009, "Design of a Multifunctional PLGA Nanoparticulate Drug Delivery System: Evaluation of Its Physicochemical Properties and Anticancer Activity to Malignant Cancer Cells," Pharm. Res., **26**, pp. 1162–1171.

[4] Tamura, T., Kita, T., Nakagawa, T., Endo, T., Kim, T. S., Ishihara, T., Mizushima, Y., Higaki, M., and Ito, J., 2005, "Drug Delivery to the Cochlea Using PLGA Nanoparticles," Laryngoscope, **115**, pp. 2000–2005.

[5] Ge, X., Jackson, R. L., Liu, J., Harper, E. A., Hoffer, M. E., Wassel, R. A., Dormer, K. J., Kopke, R. D., and Balough, B. J., 2007, "Distribution of PLGA Nanoparticles in Chinchilla Cochleae," Otolaryngol.-Head Neck Surg., **137**, pp. 619–623.

[6] Goycoolea, M. V., and Lundman, L., 1997, "Round Window Membrane. Structure Function and Permeability: A Review," Microsc. Res. Tech., **36**, pp. 201–211.

[7] Hoffer, M. E., Allen, K., Gottshall, K., Moore, R., Kopke, R. D., Wester, D., and Balaban, C., 2002, "The Early Kinetics of Gentamicin Uptake Into the Inner Ear," Int. Tinnitus J., **8**(1), pp. 27–29.

[8] Kopke, R. D., Hoffer, M. E., Wester, D., O'Leary, M. J., and Jackson, R. L., 2001, "Targeted Topical Steroid Therapy in Sudden Sensorineural Hearing Loss," Otol. Neurotol., **22**, pp. 475–479.

[9] Mondalek, F. G., Zhang, Y. Y., Kropp, B., Kopke, R. D., Ge, X., Jackson, R. L., and Dormer, K. J., 2006, "The Permeability of SPION Over an Artificial Three-Layer Membrane Is Enhanced by an External Magnetic Field," Nanobiotechnology, **4**, pp. 4–12.

[10] Barnes, A. L., Wassel, R. A., Mondalek, F., Chen, K., Dormer, K. J., and Kopke, R. D., 2007, "Magnetic Characterization of Superparamagnetic Nanoparticles Pulled Through Model Membranes," Biomagn. Res. Technol., **5**, pp. 1–10.

[11] Pasternak, A. S., and Miller, W. M., 1996, "Measurement of Trans-Epithelial Electrical Resistance in Perfusion: Potential Application for In Vitro Ocular Toxicity Testing," Biotechnol. Bioeng., **50**, pp. 568–579.

[12] Eley, J. G., Pujari, V. D., and McLane, J., 2004, "Poly (Lactide-co-Glycolide) Nanoparticles Containing Coumarin-6 for Suppository Delivery: In Vitro Release Profile and In Vivo Tissue Distribution," Drug Deliv., **11**, pp. 255–261.

[13] Kopke, R. D., Wassel, R. A., Mondalek, F., Grady, B., Chen, K., Liu, J., Gibson, D., and Dormer, K. J., 2006, "Magnetic Nanoparticles: Inner Ear Targeted Molecule Delivery and Middle Ear Implant," Audiol. Neuro-Otol., **11**, pp. 123–133.

[14] Shapiro, B., Probst, R., Potts, H. E., Diver, D. A., and Lubbe, A. S., 2007, "Control to Concentrate Drug-Coated Magnetic Particles to Deep-Tissue Tumors for Targeted Cancer Chemotherapy," Proceedings of the 46th IEEE Conference on Decision and Control, Vol. 46, pp. 3901–3906.

[15] Paulson, D. P., Abuzeid, W., Jiang, H., Oe, T., O'Malley, B. W., and Li, D., 2008, "A Novel Controlled Local Drug Delivery System for Inner Ear Disease," Laryngoscope, **118**, pp. 706–711.

[16] Coleman, J. K., Littlesunday, C., Jackson, R., and Meyer, T., 2007, "AM-111 Protects Against Permanent Hearing Loss From Impulse Noise Trauma," Hear. Res., **226**, pp. 70–78.

[17] Plontke, S. K., Biegner, T., and Kammerer, B., 2008, "Dexamethasone Concentration Gradients Along Scala Tympani After Application to the Round Window Membrane," Otol. Neurotol., **29**, pp. 401–406.

[18] Sheppard, W. M., Wanamaker, H. H., and Pack, A., 2004, "Direct Round Window Application of Gentamicin With Varying Delivery Vehicles: A Comparison of Ototoxicity," Otolaryngol.-Head Neck Surg., **131**, pp. 890–896.

[19] Lee, K. Y., Nakagawa, T., and Okano, T., 2007, "Novel Therapy for Hearing Loss: Delivery of Insulin-Like Growth Factor 1 to the Cochlea Using Gelatin Hydrogel," Otol. Neurotol., **28**, pp. 976–981.

[20] Wassel, R. A., Grady, B. P., Kopke, R. D., and Dormer, K. J., 2007, "Dispersion of Super Paramagnetic Iron Oxide Nanoparticles in Poly(D,L-Lactide-co-Glycolide) Microparticles," Colloids Surf., A, **292**, pp. 125–130.